ACADEMIA ROMÂNĂ
Revue Roumaine de Chimie
https://www.icf.ro/rrch/

Rev. Roum. Chim.,
2023, *68*(7–8), 371–381
DOI: 10.33224/rrch.2023.68.7-8.06

GREEN INHIBITION OF COPPER CORROSION BY AMMOIDES VERTICILLATA OIL IN 1M NITRIC ACID: WEIGHT LOSSAND RAMAN SPECTROSCOPIC MAPPING STUDIES

Naziha CHABANE,[a] Fayçal DERGAL,[a,b,*] Tarik ATTAR,[c,d] Nadia BELARBI,[b,e] Ilyas CHIKHI,[a,f] Samir CHERIGUI,[a,f] Mohamed Abou MUSTAPHA,[b] Djahida LERARI[b] and Khaldoun BACHARI[b]

[a]Laboratory of Catalysis and Synthesis in Organic Chemistry BP 119, University of Tlemcen, Algeria
[b]Center for Scientific and Technical Research in Physico-chemical Analyzes (CRAPC). BP 384, industrial zone 42004 Tipaza, Algeria
[c]Higher School of Applied Sciences of Tlemcen, BP 165, 13000 Bel Horizon, Tlemcen, Algeria
[d]Laboratory of Toxicomed, University Abou Beker BelkaidTlemcen, BP119, 13000 Tlemcen, Algeria
[e] Laboratory of Spectrochemistry and Structural Pharmacology, Department of Chemistry, Faculty of Sciences, University Abou BekrBelkaid Tlemcen, BP 119 Imama, 13000 Tlemcen, Algeria
[f]Belhadj Bouchaib University, BP 284, 46000 Ain Temouchent, Algeria

Received January 19, 2023

The present study was designed to predict and analyse the effect of the essential oil of Ammoides verticillata (A.E.O) originating from the city of Souahlia (Tlemcen), which is located in northwest Algeria and its major compound on the inhibition of copper corrosion in 1 M HNO_3. According to the analysis gas chromatography coupled to mass spectrometry (GC-MS), the essential oil studied is dominated by carvacrol (67.89%). The effect of concentration and temperature on the corrosion behaviour of copper and the inhibitory efficiency has been studied by the gravimetric method. The results obtained show that A.E.O and carvacrol alone present a good inhibition for copper in 1 M HNO_3. The inhibitory efficiency reaches a maximum value of 63% at 1.5 g/L for A.E.O and 79% at 0.1 g/L for carvacrol. The adsorption of A.E.O and carvacrol alone on the copper surface follows the Langmuir and Frumkin isotherm respectively. Synergy parameter proves that there is a competitive adsorption between iodide ions and A.E.O. The immersed copper surface was analysed by Raman spectroscopy.

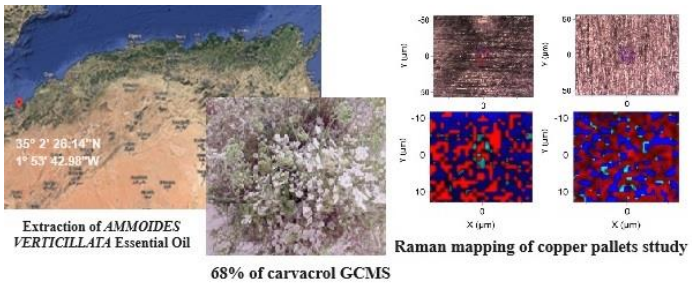

INTRODUCTION

Copper is used extensively in installations, electronics, the marine industry, electrical connectors and heat exchangers due to its mechanical resistance and excellent heat and electrical conductivity.[1,2] At the industrial level, the cleaning process of the devices is carried out with the help of acid solutions that act as corrosive agents, so it is necessary to minimize the destructive effect of acids on these devices.[3] A crucial environmental, economic, and safety issue is corrosion. It has an impact on a variety of structures, particularly metallic ones. This is one of the key reasons why most installations and pieces of equipment are altered and destroyed.[4] The inhibition of copper corrosion by organic compounds is one of the major objectives of many researchers.[5–7] Organic compounds possessing oxygen, nitrogen, phosphorus and sulfur have been

* Corresponding author: dergalf@yahoo.fr

employed extensively as organic inhibitors.[8–11] However, the majority of them are extremely harmful to both humans and the environment. Due to these harmful impacts, natural anti-corrosion treatments that are safe for the environment are now being used.[12] Green inhibitors such as plant extracts[13] and oils have emerged as significant, readily available, environmentally acceptable and renewable sources for a variety of inhibitors.[14] Their richness by different types of organic compounds presents a good inhibiting efficiency.[15] Depending on the location and the part of the plant employed, both the yield of these natural substances and the potential to inhibit corrosion vary greatly.[16] Because of their biodegradability, their ecological character and their low cost,[17–19] several studies have been devoted to the green inhibition of the corrosion of metals by essential oils. The study of Belarbi *et al*.[14] on the use of *L. Stoechas* oil as a corrosion inhibitor for steel in 1 M HCl medium indicated that the oil gave a good inhibition efficiency of 61.97% at 2 g/L oil at 30°C, Belarbi *et al*.[4] also conducted a study on the influence of *Ammodaucus Lecotrichus* on copper corrosion in 2 M HCl solution, the results revealed an efficiency of 70% for a concentration of 3000 ppm at 25 °C. The use of the essential oil of *Pistacialentiscus* by Dahmani *et al*.[20] showed a very important inhibiting action against copper corrosion.

Since ancient times, *A. verticillata* has been well known for its applications in self-medication. It is used to treat bronchial issues, an absence of appetite, and digestive ailments, it has antifungal, antiviral, antimicrobial and antiaggregant properties and activities.[21,22] In this paper, we were interested in studying the inhibitory performance of *A. verticillata* oil and its major compound on copper corrosion in 1 M HNO_3, we also studied the synergistic effect of KI on *A. verticillata* oil using gravimetric method and Raman spectroscopy, with mapping one of the techniques used to identify the distribution of the corroded zone with inhibited zones.

Raman mapping is used Raman in various fields such as the characterization of materials, bacteria, polymers and for the characterization of copper corrosion products by determining their respective mass fraction. In this work, we propose a new method for the phase the identification and determination of the relative abundance of the corroded components, using the characteristic Raman bands of the copper phases present in the corroded one. which allowed us to have the distribution of the two phases by mapping and thus to be able to see the effect of the inhibition of our materials.[23–26]

EXPERIMENTAL PART

Preparation of inhibitors

Ammoides verticillata essential oil

The samples of *A. verticillata* (aerial part) were collected in June 2021 in the province of Souahlia in the northwest of Tlemcen (Fig. 1). The station's relative GPS coordinates are 35°2'26.14"N latitude and 1°53'42.98"W longitude. The plant Material was dried for four months at ambient temperature before being hydro distilled by a Clevenger-type device for 3 h. Using anhydrous sodium sulfate, *A. verticillata* oil (A.E.O) was dehydrated before being preserved at 4°C in sealed glass vials.

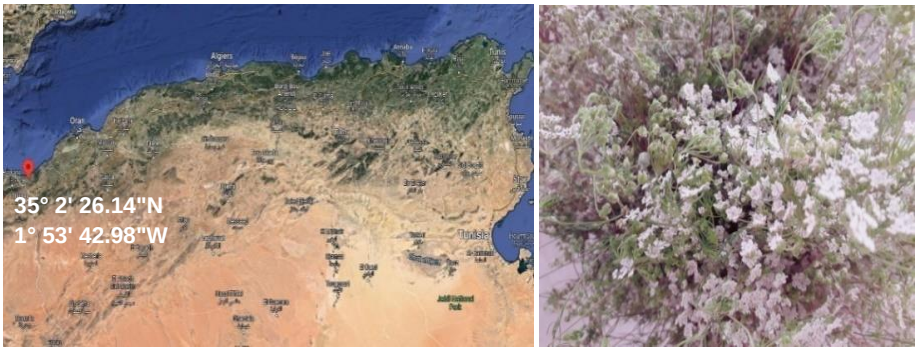

Fig. 1 – Image of the plant, GPS coordinates and map of the plant's area.

Carvacrol

The fractionation of the essential oil of *A. verticillata* to obtain the carvacrol was carried out with a column of chromatography on silica gel using a mixture of hexane and ethyl acetate solvents. The Chromatography of the essential oil is performed by diluting three (03) drops of the oil in 1 mL of DCM. The same operation is performed with pure carvacrol. With the help of a capillary, each sample is placed on a silica plate, hexane/ethyl-acetate, the eluent used in this operation. After a few minutes, the plate is removed, dried and passed to the UV. Chromatography on silica gel is based on the same principles as CCM with the difference that the migration of the compounds is done by gravity. The fractions were obtained using amixture of the hexane/ethyl-acetate (96/4). The structure of carvacrol after separation was confirmed by proton ^{1}H-NMR.

Gravimetric corrosion tests

In this study we employed commercial pure copper in a 1M HNO_3 solution. The surface of the copper specimen is pre-treated by polishing with various abrasives (from 360 to 1000 grains), washing with double distilled water and then with acetone, drying and weighing before being plunged to the freshly prepared test solution. The temperature of the medium is maintained at 298 K. After the tests, the specimens were cleaned, dried and weighted by an analytical balance. All measurements were carried out in triplicate and the average value of the weight loss was noted. The synergistic impact of KI (10^{-3} M) on the oil of *A. verticillata* was studied at different temperatures.

The inhibitory action of A.E.O and its majority compound on copper corrosion at 298 K in 1M HNO_3 was evaluated gravimetrically after 3 h of immersion. The action of different concentrations of A.E.O (from 0.25 to 1.5 g/L) and carvacrol alone (from 0.1 to 0.6 g/L) on the inhibition potential was studied.

The corrosion rate (1), the inhibitor efficiency (2) and the surface coverage of the inhibitor (3) are calculated by the following relations:[27]

$$CR = (m_i - m_f)/t \times S \quad (1)$$

where m_i and m_f are the initial and final mass of the specimen, t symbolizes the immersion time and S represents the total area of the specimen.

$$IE\ [\%] = 100 \times (CR_0 - CR_{inh})/CR_0 \quad (2)$$

$$\Theta = 1 - (CR_{inh} / CR_0) \quad (3)$$

where CR_0 and CR_{inh} are the corrosion rates in the absence and the presence of the inhibitor, respectively.

RAMAN and NMR spectroscopies

Raman spectroscopic investigation were performed using a HORIBA LABRAM HR Raman spectrometer operated in single spectrograph mode with a holographic dispersive grating of 600 grooves/mm equipped with a frequency (325, 633 and 785 nm). The samples were analyzed in the back-scattering mode on the microscope stage of an Olympus confocal microscope attached to the spectrometer using a long working distance 50× and 100 × objective. The detector used was a liquid nitrogen cooled charge coupled device Symphony IGA detector. A 663 and 785 nm holographic notch filter were used to remove the Rayleigh-scattered light. The entrance slit width was 100 μm giving a resolution of 2 cm^{-1} in the range between 100 and 5000 cm^{-1}. Repeated acquisition using the highest magnification were accumulated to improve the signal to noise ratio in the spectra. Spectra were calibrated using the 520.5 cm^{-1} line of a silicon wafer. NMR Spectroscopic investigation were performed using a MAGRITEK SPINSOLVE 60 CARBON spectrometer. The permanent magnetic produced a magnetic field of 1 T (42 MHz 1H Larmor frequency) with a homogeneity of about 0.01 ppm across the 5 mm diameter sample tube in $CDCl_3$ solvent, which completely filled the solenoidal radio-frequency coil. The signal to noise ratio of a single-scan spectrum for a water sample was about 200,000. NMR spectra of the pure solution flowing through the magnet were measured every 10–15 s depending on the case.

RESULTS AND DISCUSSION

Ammoides verticillata oil and carvacrol analysis

Ammoides verticillata oil composition

Twelve volatile compounds that accounted for 98.31% of the total *A. verticillata* oil were identified by GC-MS analysis. Carvacrol (67.89%) is the major compound followed by γ-Terpinene (16.6%) and p-Cymene (7.99%) (Table1). A study was conducted by Hanane Senouci *et al*. on the oil of *A. verticillata* from Beni Snous near the city of Tlemcen (Algeria), found that the oil is rich in carvacrol (44.3%), limonene (19.3%) and p-cymene (19.2%).[28]

Table 1

Chemical composition of Ammoides verticillata essential oil

N°	Compounds [a]	RI_a [b]	RI_a [e]	%	Identification
1	Moslene	1030	910	0.12	RI, MS
2	α-Pinene	917	913	0.18	RI, MS
3	β-Pinene	952	940	0.26	RI, MS
4	α-Terpinene	1003	953	0.33	RI, MS
5	p-Cymene	992	959	7.99	RI, MS
6	Limonene	995	960	1.63	RI, MS
7	γ-Terpinene	1030	978	16.6	RI, MS
8	α- Phellandrene	1010	1041	0.38	RI, MS
9	β-Phellandrene	1010	1043	0.08	RI, MS
10	Thymol methyl ether	1235	1117	2.61	RI, MS
11	Carvacrol methyl ether	1245	1120	0.24	RI, MS
12	Carvacrol	1298	1111	67.89	RI, MS
Total identification (%)				98.31	

[a] Order of elution are given on the apolar (HP-5MS) column,

[b] Retention indices of literature on the apolar column (RI_a) reported from the literature,

RI^e – Retention Indices;

MS – Mass Spectrometry in electronic impact mode.

The ^{1}H NMR of carvacrol

The proton NMR spectrum of carvacrol was recorded on a SPINSOLVE 60 CARBON spectrometer. The experiment was performed at 25°C using $CDCl_3$ to prepare the carvacrol sample and TMS as internal standard (Fig. 2).

The ^{1}H NMR spectrum of carvacrol purafter separation shows the chemical shifts: 1.25 ppm (d, $6H_a$); 2.3 ppm (s, $3H_e$); 2.9 ppm (m, $1H_b$); 5.28 ppm (s, $1H_d$); 6.73 ppm (s, $1H_c$); 6.88 ppm (d, $1H_f$); 7.1 ppm (d, $1H_g$).

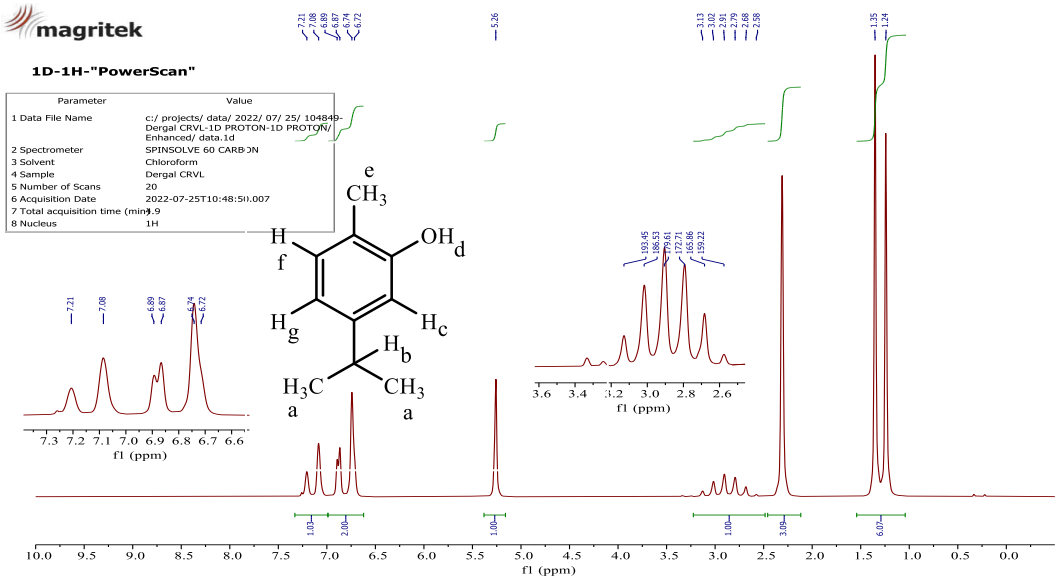

Fig. 2 – The proton NMR spectrum of carvacrol.

Corrosion measurement

Concentration effect

The anticorrosive performance of A.E.O and carvacrol alone against corrosion was investigated by monitoring the weight loss during the process. The weight loss was determined in nitric acid in the absence and presence of different concentrations of the both inhibitors during a three-hour immersion period.

According to Table 2, the inhibitory action improves with the addition of A.E.O in the medium to reach an optimal efficiency of 63.13% at 1.5 g/L. But this is not the case for the majority compound where the inhibitory action decreases with the increase of carvacrol concentration in the aggressive medium. The results from the Table 3 show that the corrosion rate increases with increase in the concentration of carvacrol in nitric acid and the maximum surface coverage is found to be 0.79 at 0.1 g/L. The inefficiency above 0.1 g/L may be due to weakening of metal-inhibitor interactions, resulting in the replacement of inhibitor by nitrate ions or water with decrease in inhibition efficiency.

Table 2

Rate of corrosion of the dissolution of copper in 1 M HNO_3 at different concentrations of A.E.O for 3 h at 25°C

Inhibitor Concentration [g/L]	CR [mg·cm^{-2}·h^{-1}]	IE [%]	θ
0	0.3385	–	------
0.25	0.2468	27.09	0.27
0.5	0.1822	46.17	0.46
1	0.1515	55.24	0.55
1.5	0.1248	63.13	0.63

The comparison between the results summarized in Tables 2 and 3 informs us that carvacrol alone inhibits better than its presence in the essential oil of *A. Verticillata*. For example, the highest inhibition value is 79.88% at 0.1g/L of the majority compound concentration which corresponds to an inhibition of

27.09% at 0.25g/L of the A.E.O concentration. This can be explained by the presence of a competitive effect between carvacrol and other organic compounds of A.E.O.

Table 3

Rate of corrosion of the dissolution of copper in 1 M HNO_3 at different concentrations of carvacrol for 3 h at 25°C

Inhibitor Concentration [g/L]	CR [mg·cm^{-2}·h^{-1}]	IE [%]	θ
0.0	0.3385	------	------
0.1	0.0681	79.88	0.79
0.2	0.1284	62.06	0.62
0.4	0.1897	43.95	0.43
0.6	0.2228	34.18	0.34

Effect of temperature on inhibitor activity and thermodynamic parameters

Generally, the rise in temperature reduces the stability of metals because it accelerates the speed of its degradation and thus loses their physical-chemical properties. However, the influence of the temperature differs according to the corrosive environment where the material is located.[29] The impact of temperature on the inhibition of copper corrosion was determined after 3h of immersion in 1M HNO_3in the absence and existence of inhibitor at a concentration of 1.5 g/L for essential oil and 0.1 g/L for carvacrol.

It can be clearly seen from Table 4 that the inhibitory efficiency of A.E.O and carvacrol alone decreases with increasing temperature. This decrease can be justified by the desorption of organic molecules of the inhibitor adsorbed on the surface of copper specimen at higher temperature.[30,31]

The high speed of dissolution of copper in nitric acid solution at elevated temperature may be assigned to the corrosive agent acquiring higher dissolution energy in the aggressive solution.[31]

The Arrhenius equation may be employed to demonstrate the impact of temperature on inhibitor performance.[32]

$$\ln (CR) = (-E_a/RT) + A \qquad (4)$$

where CR stands for speed of corrosion of copper, E_a denotes the activation energy (kJ mol^{-1}), R represents the gas constant (8.314 J mol^{-1} K^{-1}), T is the temperature (K), and A refers to Arrhenius pre-exponential factor.

Table 4

Gravimetric results of copper corrosion in 1M HNO_3without and with 1.5 g/L of A.E.O and 0.1 g/L of carvacrol at different temperatures

	A.E.O (1.5 g/L)			*Carvacrol (0.1 g/L)*		
T [K]	CR_0	CR_{inh}	IE [%]	CR_0	CR_{inh}	IE [%]
298	0.3385	0.1248	63.13	0.3385	0.0681	79.88
308	0.6556	0.2998	54.26	0.6556	0.1675	74.45
318	1.4755	0.7672	48.00	1.4755	0.4368	70.39
328	3.1927	2.4429	23.48	3.1927	1.6171	49.35

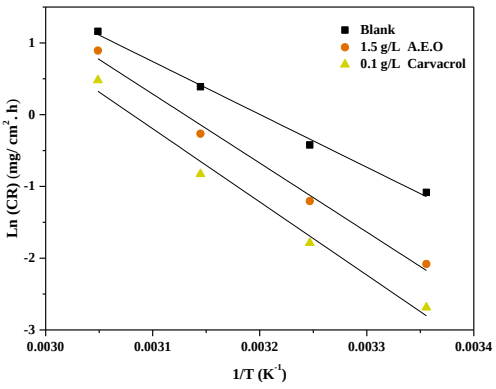

Fig. 3 – Arrhenius charts for corrosion of copper in 1M HNO_3 without and with 1.5 g/L of A.E.O and 0.1 g/L of carvacrol.

The E_a values (Table 5) for copper in 1 M HNO_3 in the absence and existence of A.E.O (1.5 g/L) and carvacrol alone (0.1 g/L) inhibitors were determined from the slope of the curve of ln(CR) = f (1/T) (Fig. 3).

The enthalpy ΔH_a, entropy ΔS_a and free-energy ΔG_a values (Table 5) can be determined by Equations (5) and (6).[33,34]

$$\mathrm{CR} = \frac{RT}{Nh}\exp\left(\frac{\Delta S_a}{R}\right)\exp\left(-\frac{\Delta H_a}{RT}\right) \quad (5)$$

$$\Delta G_a = \Delta H_a + T\,\Delta S_a \quad (6)$$

where N is Avogadro's number, h is the universal Plank's constant and R is the gas constant.

The ΔH_a and ΔS_a values were determined from the curve ln (CR/T) = f (1/T), which represents a straight line (Fig. 4) where ($-\Delta H_a/R$) and [ln(R/Nh) + ($\Delta S_a/R$)] presents the slope and intercept, respectively.

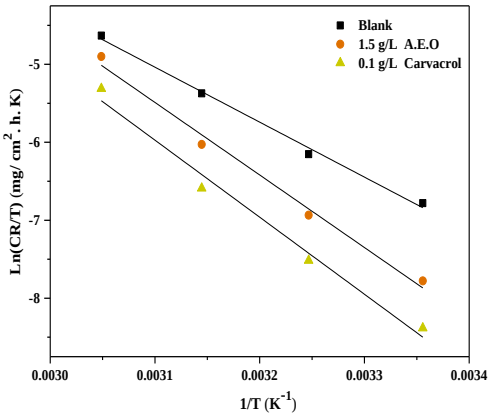

Fig. 4 – Transition state charts for corrosion of copper in 1M HNO_3 without and with 1.5 g/L of A.E.O and 0.1 g/L of carvacrol.

According to the results grouped in Table 5, E_a of medium inhibited by A.E.O and carvacrol alone is greater than that of the uninhibited medium indicating a physisorption mode.[35,36] This effect may be assigned by the double layer's thickness raising the energy barrier, which reduces copper's speed of corrosion in the existence of inhibitor.[37,38] On the other hand, organic inhibitors have the ability to combine with a metal to produce a metal-inhibitor complex, which raises the activation energy and slows the corrosion process.[37,39] Whatever the medium, the ΔH_a values were higher than zero, which shows that the dissolution nature of the metal is endothermic.This means that the dissolution of copperis slow.[4,40,41] Without an inhibitor, the high negative value of ΔS_a means that the activated complex is the speed determining stage, instead of the dissociation stage.[31] While in the presence of A.E.O, the value of entropy raises, which implies that an increase in disorder due to the formation of activated complexes.[31] The positive entropy value in the presence of carvacrol means that the complex activated in the speed determining stage represents dissociation instead of association, indicating that disorder raises on starting from reactants to the activated complex.[31] The positive value of ΔG_a indicates a non-spontaneous corrosion reaction. These values of ΔG_a are due to the formation of unstable activated complex in the rate determining transition state. Moreover, the higher values of ΔG_a of the process in both inhibitors presence when compared to that in its absence is attributed to its physisorption, while the opposite one is the case with chemisorption.[42]

Table 5

Thermodynamic activation parameters for copper corrosion in 1M HNO_3 without and with A.E.O (1.5 g/L) and carvacrol alone (0.1g/L) using Arrhenius and transition state plots

Inhibitor [g/L]	E_a [kJ·mol^{-1}]	ΔH_a [kJ·mol^{-1}]	ΔS_a [J·mol^{-1}·K^{-1}]	$\Delta G_{a(313K)}$ [kJ·mol^{-1}]
0	61.21	58.61	–57.64	77.78
A.E.O	79.95	77.35	–3.29	78.33
Carvacrol	84.74	82.14	7.54	79.89

Adsorption isotherm

The green inhibition of metal corrosion by essential oils rich in different types of organic compounds, such as terpenes and flavonoids are explained by the adsorption of these compounds on the metal surface. There are several parameters that influence the chemical or physical nature of the adsorption of the inhibitor, such as the nature and the charge of the metal itself, the structure of the organic compounds of the inhibitor and also the type of electrolyte.[14] In order to characterize the appropriate adsorption isotherm for this study, different isotherm types including Langmuir, El-Awady, Temkin, Frundlich, Flory-Huggins and Frumkin were tested. The Langmuir isotherm provides the most accurate description for A.E.O (Fig. 5) and Frumkin isotherm turns out to be the best fit for carvacrol alone (Fig. 6). These isotherms can be stated as follows:

Langmuir adsorption isotherm:[4,43]

$$\frac{C_{inh}}{\theta} = \frac{1}{K_{ads}} + C_{inh} \qquad (7)$$

Frumkin adsorption isotherm:[3]

$$\ln\left(\frac{\theta}{(1-\theta)\times C}\right) = \ln K_{ads} + 2a\theta \qquad (8)$$

where C_{inh} is the inhibitor concentration [g/L], K_{ads} symbolizes the adsorption equilibrium constant and a is the interaction parameter of molecules.

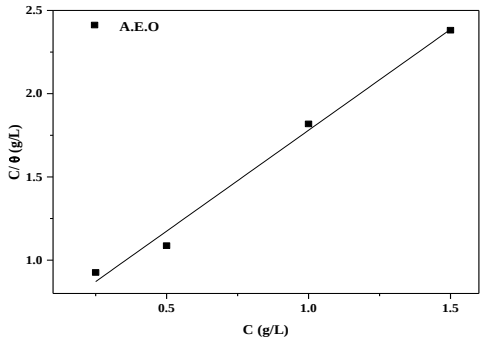

Fig. 5 – Langmuir isotherm for A.E.O adsorption on copper in 1M HNO_3 solutionat 25°C.

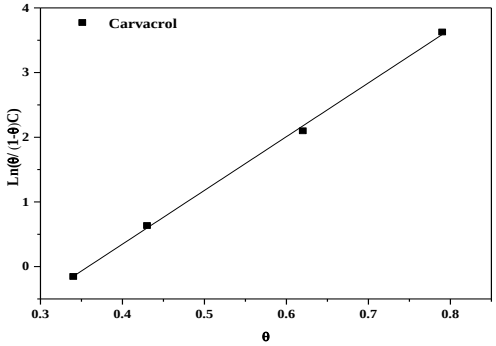

Fig. 6 – Frumkin isotherm for carvacrol adsorption on copper in 1M HNO_3solution at 25°C.

These figures show a line demonstrating that the adsorption of A.E.O and carvacrol alone follows the Langmuir and Frumkin isotherm, respectively. The correlation coefficients (R^2) are nearly to 1. The values of K_{ads} and R^2 were obtained from the Langmuir and Frumkin isotherms (Figs. 5 and 6) and reported in Table 6.

K_{ads} equilibrium constant is connected to the ΔG_{ads} free standard energy by the equation (9);[4,14,44]

$$\Delta G^{\circ}_{ads} = -RT\ln(K_{ads} \times C) \qquad (9)$$

where C is the water concentration (103g/L), R symbolizes the perfect gases constant (J/ mol·K) and T is the temperature (K).

The values of the equilibrium constant K_{ads} for both inhibitors are positive, signifying the feasibility of inhibitors adsorption to the copper surface.[10] On the other hand, the ΔG_{ads} values are around –20 KJ/mol for the two inhibitors studied, which shows that there is a physisorption of the inhibitor on the copper surface in a solution of 1 M nitric acid at 25°C by electrostatic interactions between the copper surface charges and the inhibitor molecules.[3] The negative value of ΔG_{ads} confirmed the spontaneity of its process and the stability of the protective film formed on the copper sample surface.[16,21]

Table 6

Thermodynamic parameters for adsorption of two inhibitors on copper tested in a 1M HNO_3 solution at 25°C

Inhibitor [g/L]	R^2	K_{ads} [L/g[	ΔG_{ads} [KJ·mol^{-1}[
A.E.O	0.986	1.7599	–18.51
Carvacrol	0.998	0.0510	–9.74

Synergistic effect

Utilizing the notion of synergism and using a combination of inhibitors is one potential way to boost the corrosion inhibition efficiency cost-effectively.[46] The phenomena of synergism in corrosion inhibition this translates into an increase in the inhibitors ability to resist corrosion in the existence of secondary compounds in aggressive

solution.[47] The existence of halide ions, such as chloride, bromide and iodide in acid solution including organic inhibitors turned out to stabilize the adsorption process of organic cations, producing an increase in the efficacy of inhibition.[48] Due to its size and ease of polarization, iodide showed a bigger synergistic impact than chloride and bromide.[49] In this part, we will study the impact ofKI (10^{-3}M) on the efficiency of copper corrosion inhibition in 1M HNO_3 in presence of 1.5 g/L of *Ammoides verticillate* oil at different temperatures. The calculation of synergistic parameter (S_θ) which is expressed as follows:[3,50]

$$S_\theta = (1 - \theta_{A.E.O + KI}) / (1 - \theta'_{A.E.O + KI}) \quad (10)$$

$$\theta_{A.E.O + KI} = (\theta_{A.E.O} + \theta_{KI}) - (\theta_{A.E.O} * \theta_{KI}) \quad (11)$$

where $\theta_{A.E.O}$ and θ_{KI} are the surface coverage by A.E.O and KI, respectively and $\theta'_{A.E.O + KI}$ is the surface coverage by A.E.O in combination with KI.

S_θ is bigger than 1 when there is a synergistic impact between A.E.O and KI, while it is nearly to 1 if there is no interaction between the selected inhibitors and lower than 1 if there is an antagonistic impact that produces competitive adsorption.[51] Table 7 groups the synergistic parameter S_θ values for 1.5 g/L A.E.O in combination with KI.

It is clear from Table 7 that all values S_θ are smaller than unity. This finding indicates that a competitive adsorption between A.E.O and KI.

Table 7

Synergism parameter S_θ for A.E.O (1.5 g/L) in the presence of 10^{-3}M of KI from gravimetric measurements at 298, 308 and 318 K

	A.E.O. [1.5 g/L]	KI [10^{-3} M]	A.E.O. [1.5 g/L] + KI [10^{-3} M]	
T (K)		IE / %		S_θ
298	63.13	56.04	71.37	0.56
308	54.26	61.53	57.79	0.41
318	48.00	63.22	48.80	0.37

Raman Spectroscopy analysis

The Electronic Microscopy of the Raman (Fig. 7) of the surfaces of copper samples were taken at same magnification to see the changes that occurred during corrosion process in the absence and presence of Ammoides verticillata oil (1.5 g/L), carvacrol alone (0.1 g/L) and KI (10^{-3}M) with A.E.O (1.5 g/L) during 3 h at 25 °C.

The EM image of the copper specimen in the absence of the inhibitor shows an irregular and damaged surface owing to rapid corrosion attack if we compare that with pure copper (Fig. 7). However, a relatively smoother and less corroded morphology of copper surface can be observed in the presence of inhibitor (essential oil and carvacrol alone), this effect deteriorates in the presence of KI (Fig. 7e). This may be intercepted by the adsorption of molecules of this inhibitor on the electrode surface. It is thought that the molecules of inhibitor depress the corrosion by the formation of an adherent deposit on the electrode surface limiting the access of the electrolyte to the surface of the copper. These results are in agreement with the inhibition efficiency obtained from the weight loss measurement.

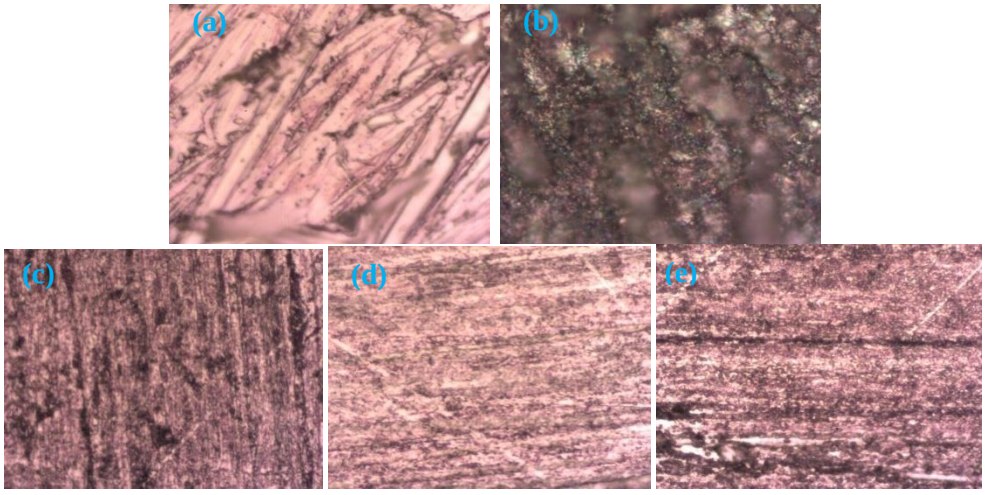

Fig. 7 – Raman Electronical microscopy morphologies of: a) copper; b) in 1 M HNO_3; c) 1 M HNO_3 + 1.5g/L of *Ammoides verticillata* essential oil; d) 1 M HNO_3 + 0.1 g/L of carvacrol; e) 1 M HNO_3 + 1.5 g/L *Ammoides verticillata* essential oil with *KI* for 3 h immersion (magnification ×100).

Figure 8 show the Raman spectra of copper, tree characteristic peaks of Cu_2O are observed at 97, 147, 615 cm^{-1} in the spectrum of copper plates. The Raman microscope make possible to do spectra by targeting the oxidized parts and the pure parts. We observe in the zone (1) the characteristic spectrum of copper with two peaks 615 cm^{-1}, for the oxidized zones (2) we observe the appearance of peaks at 1370 and 1578 cm^{-1} due to the deposition of a thin layer of carbon on the surface on areas not inhibited by essential oils, these two peaks are observed in the presence of KI but with a very low intensity.[52,53]

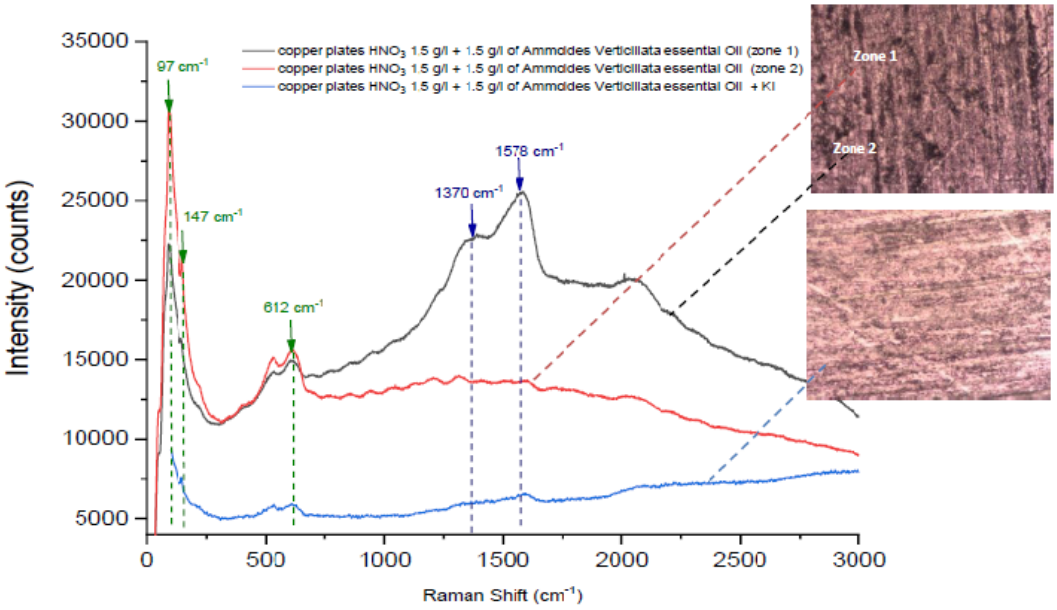

Fig. 8 – Raman spectra of copper 1 M HNO_3 + 1.5 g/L of *Ammoides verticillata* essential oil (zone 1), copper 1 M HNO_3 + 1.5 g/L of *Ammoides verticillata* essential oil (zone 2*)* and copper 1 M HNO_3 + 1.5 g/L *Ammoides verticillata* essential oil with KI for 3 h immersion.

We provide a Raman mapping of our copper plates which were put in an aggressive 1M HNO_3 medium in the presence of inhibitor (essential oil, carvacrol alone and essential oil with KI), Fig. 9, the mapping will help us to see the distribution of the oxidized parts compared to the inhibited parts and thus see the effect of carvacrol when it is present in the essential oil and when it is pure, thus allowing us to confirm the effect synergy on corrosion inhibition.

These maps will allow us to see the distribution of the corroded parts on the copper plate and to see the effect of the inhibitor by delimiting the areas having been attacked by the acid and the areas inhibited by our essential oil. The Electronic Microscopy morphology of copper in HNO_3 and A.E.O show two different kind of area we choose we have chosen an area comprising the two colors of our copper plate with a number of points to make our mapping of 164 cm^{-1} in order to have a number of Raman spectra covering the entire area. The spectra show the presence of two spectra the first areas for which we have chosen a red color and a second area corresponding to the appearance of the peaks at 1370 and 1578 cm^{-1} due to the deposition of a thin layer of carbon. If we compare the distribution of the two given zones compared to the results obtained by gravimetry, we observe the same ratio which corresponds to 63% of inhibition with just essential oil (Fig. 9A).

As shown by gravimetry, the mapping with only carvacrol as an inhibitor increases the inhibition rate to 79%, this increase is reflected in the Raman mapping by an increase in the copper zone given by the red color and a decrease in the bands given in blue color, this result shows the increase of the inhibitory effect in the presence of carvacrol and confirms the results obtained by gravimetry, carvacrol has good inhibition alone than in the presence of other terpenes in the essential oil. The mapping with the presence of KI with A.E.O shows the increases the inhibition rate to 71%, this increase is reflected in the Raman mapping by a increase in the copper zone given by the red color and a decrease in the bands given in blue color, this result shows the increase of the inhibitory effect in the presence of KI and confirms the results obtained by gravimetry.

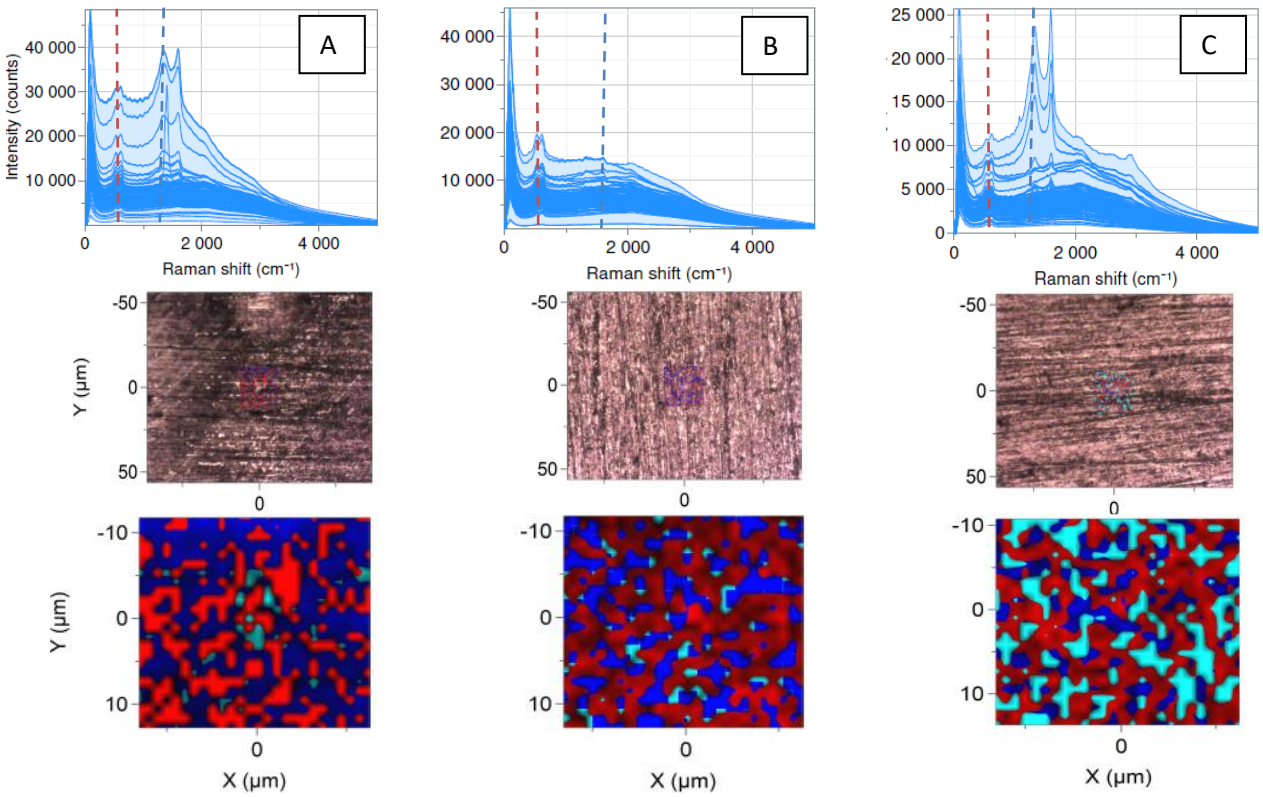

Fig. 9 – Raman mapping of copper pallets in: A) 1 M HNO_3 + 1.5 g/L of *Ammoides verticillata* essential oil; B) 1 M HNO_3 + 0.1 g/L of carvacrol and C) 1 M HNO_3 + 1.5 g/L of *Ammoides verticillata* essential oil with KI.

CONCLUSION

The main conclusions of this study may be summarized as follows. The essential oil of *Ammoides verticillata* and its major compound may be used as a green inhibitor of copper corrosion in 1 M HNO_3 with good efficiency of 63.13% and 79.88%, respectively.

The major compound alone inhibits better than its presence in the essential oil which implies the absence of synergy between the major compound and the other organic compounds of essential oil. The rise in temperature negatively affects the inhibitory efficiency of A.E.O and its majority compound.

The adsorption of A.E.O. and major compound alone on the copper surface follows the Langmuir and Frumkin isotherm, respectively. The value of the Gibbs free energy of adsorption suggested that the both inhibitor molecules have been spontaneously adsorbed onto the copper surface through a physical adsorption mechanism.

The addition of iodide ions to A.E.O. increases the effectiveness of the inhibitor. The mapping clearly represents the distribution of corroded versus A.E.O. inhibited sections with an increase in inhibition in the case of majority compound alone. The spectra and Raman mapping are in good agreement with the results obtained by the gravimetric method.

REFERENCES

1. K. Krishnaveni and J. Ravichandran, *J. Electroanal. Chem.*, **2014**, *735*, 24–31.
2. I. Vargas, D. Fischer, M. Alsina, J. Pavissich, P. Pastén and G. Pizarro, *Materials*, **2017**, *10*, 1036.
3. N. Sait, N. Aliouane, N. Ait Ahmed, L. Toukal and M. Al-Noaimi, *J. Adhes. Sci. Technol.*, **2022**, *36*, 109–133.
4. N. Belarbi, F. Dergal, I. A. El-Haci, T. Attar, D. Lerari, B. Dahmani, C. A. Ramdane-Terbouche and K. Bachari, **2021**, *13*, 18.
5. G. Vengatesh and M. Sundaravadivelu, *J. Adhes. Sci. Technol.*, **2020**, *34*, 2075–2106.
6. H. Messaoudi, F. Djazi, M. Litim, B. Keskin, M. Slimane and D. Bekhiti, *J. Adhes. Sci. Technol.*, **2020**, *34*, 2216–2244.
7. J. Chen, Y. Qiang, S. Peng, Z. Gong, S. Zhang, L. Gao, B. Tan, S. Chen and L. Guo, *J. Adhes. Sci. Technol.*, **2018**, *32*, 2083–2098.
8. G. K. Gomma and M. H. Wahdan, *Mater. Chem. Phys.*, **1994**, *39*, 142–148.

9. M. Hrimla, L. Bahsis, A. Boutouil, M. R. Laamari, M. Julve and S.-E. Stiriba, *J. Adhes. Sci. Technol.*, **2020**, *34*, 1741–1773.
10. T. Attar, F. Nouali, Z. Kibou, A. Benchadli, B. Messaoudi, E. Choukchou-Braham and N. Choukchou-Braham, *J. Chem. Sci.*, **2021**, *133*, 109.
11. N. Sait, N. Aliouane, L. Toukal, H. Hammache, M. Al-Noaimi, J. J. Helesbeux and O. Duval, *J. Mol. Liq.*, **2021**, *326*, 115316.
12. S. Paul and I. Koley, *J. Bio- Tribo-Corros.*, **2016**, *2*, 6.
13. I. Chikhi, F. Dergal, D. M. Gana, M. E. A. Dib and H. Chaker, *J. Appl. Biotechnol. Rep.*, **2019**, *6*, 50–54.
14. N. Belarbi, F. Dergal, I. Chikhi, S. Merah, D. Lerari and K. Bachari, *Int. J. Ind. Chem.*, **2018**, *9*, 115–125.
15. S. Mo, H.-Q. Luo and N.-B. Li, *Chem. Pap.*, **2016**, 70.
16. A. Khadraoui, A. Khelifa, M. Hadjmeliani, R. Mehdaoui, K. Hachama, A. Tidu, Z. Azari, I. B. Obot and A. Zarrouk, *J. Mol. Liq.*, **2016**, *216*, 724–731.
17. A. M. Fekry, R. A. Ahmed and S. A. Bioumy, *J. Bio-Tribo-Corros.*, **2020**, *6*, 106.
18. M. Rbaa, P. Dohare, A. Berisha, O. Dagdag, L. Lakhrissi, M. Galai, B. Lakhrissi, M. E. Touhami, I. Warad and A. Zarrouk, *J. Alloys Compd.*, **2020**, *833*, 154949.
19. K. Dahmani, M. Galai, M. Ouakki, M. Cherkaoui, R. Touir, S. Erkan, S. Kaya and B. El Ibrahimi, *Inorg. Chem. Commun.*, **2021**, *124*, 108409.
20. K. Dahmani, M. Galai, A. Ech-chebab, M. Ouakki, L. Kadiri, A. Elgendy, R. Ez-Zriouli and M. Cherkaoui, *J. Appl. Electrochem.*, **2022**, *52*, 1629–1646.
21. C. Bekhechi, J. B. Boti, F. A. Bekkara, D. E. Abdelouahid, J. Casanova and F. Tomi, *Nat. Prod. Commun.*, **2010**, *5*, 1934578X1000500.
22. F. Benyoucef, M. E. A. Dib, B. Tabti, A. Zoheir, J. Costa and A. Muselli, *Anti-Infect. Agents*, **2020**, *18*, 72–78.
23. F. Dubois, C. Mendibide, T. Pagnier, F. Perrard and C. Duret, *Corros. Sci.*, **2008**, *50*, 3401–3409.
24. M. C. Mayoral, J. M. Andrés, M. T. Bona, V. Higuera and F. J. Belzunce, *Surf. Coat. Technol.*, **2008**, *202*, 5210–5216.
25. L. I. McCann, K. Trentelman, T. Possley and B. Golding, *J. Raman Spectrosc.*, **1999**, *30*, 121–132.
26. Z. Benladghem, S. M. L. Seddiki, F. Dergal, Y. M. Mahdad, M. Aissaoui and N. Choukchou-Braham, *Biofouling*, **2022**, *38*, 852–864.
27. A. Benchadli, T. Attar, B. Messaoudi and E. Choukchou-Braham, *Hung. J. Ind. Chem.*, **2021**, *49*, 59–69.
28. H. Senouci, N. G. Benyelles, M. E. Dib, J. Costa and A. Muselli, *Recent Pat. Food Nutr. Agric.*, **2020**, *11*, 182–188.
29. T. Attar, L. Larabi and Y. Harek, *Int. J. Adv. Chem.*, **2014**, *2*, 139–142.
30. G. Karthik and M. Sundaravadivelu, *J. Adhes. Sci. Technol.*, **2017**, *31*, 530–551.
31. T. Attar, A. Benchadli, B. Messaoudi, N. Benhadria and E. Choukchou-Braham, *Bull. Chem. React. Eng. Catal.*, **2020**, *15*, 454–464.
32. M. P. Chakravarthy, K. N. Mohana and C. B. Pradeep Kumar, *Int. J. Ind. Chem.*, **2014**, *5*, 19.
33. M. Mobin, S. Zehra and R. Aslam, *RSC Adv.*, **2016**, *6*, 5890–5902.
34. S. J. Khouri, *Am. J. Anal. Chem.*, **2015**, *06*, 429–436.
35. S. A. Umoren, I. B. Obot and E. E. Ebenso, *E-J. Chem.*, **2008**, *5*, 355–364.
36. M. Salah, L. Lahcène, A. Omar and H. Yahia, *Int. J. Ind. Chem.*, **2017**, *8*, 263–272.
37. H. Vashisht, I. Bahadur, S. Kumar, M. S. Goyal, G. Kaur, G. Singh, L. Katata-Seru and E. E. Ebenso, *J. Mol. Liq.*, **2016**, *224*, 19–29.
38. M. N. El-Haddad, *Int. J. Biol. Macromol.*, **2013**, *55*, 142–149.
39. Y. Qiang, S. Zhang, S. Yan, X. Zou and S. Chen, *Corros. Sci.*, **2017**, *126*, 295–304.
40. M. Faustin, A. Maciuk, P. Salvin, C. Roos and M. Lebrini, *Corros. Sci.*, **2015**, *92*, 287–300.
41. R. A. Rikkouh, T. Douadi, H. Hamani, M. Al-Noaimi and S. Chafaa, *J. Adhes. Sci. Technol.*, **2020**, *34*, 1454–1479.
42. T. Attar, A. Benchadli, B. Messaoudi, E. Choukchou-Braham, *Chem. & Chem. Technol.*, **2022**, *16*, 440–447.
43. K. Ramya, R. Mohan, K. K. Anupama and A. Joseph, *Mater. Chem. Phys.*, **2015**, *149–150*, 632–647.
44. C. K. Anyiam, O. Ogbobe, E. E. Oguzie, I. C. Madufor, S. C. Nwanonenyi, G. C. Onuegbu, H. C. Obasi and M. A. Chidiebere, *SN Appl. Sci.*, **2020**, *2*, 520.
45. M. Heydari and M. Javidi, *Corros. Sci.*, **2012**, *61*, 148–155.
46. S. Javadian, A. Yousefi and J. Neshati, *Appl. Surf. Sci.*, **2013**, *285*, 674–681.
47. R. Aslam, M. Mobin, J. Aslam and H. Lgaz, *Sci. Rep.*, **2018**, *8*, 3690.
48. U. M. Eduok, S. A. Umoren and A. P. Udoh, *Arab. J. Chem.*, **2012**, *5*, 325–337.
49. K. S. Shaju, K. J. Thomas, V. P. Raphael and A. Paul, *ISRN Corros.*, **2012**, *2012*, 1–8.
50. P. Roy, A. Pal and D. Sukul, *RSC Adv.*, **2014**, *4*, 10607.
51. O. A. Hazazi, A. Fawzy and M. Awad, *Int. J. Electrochem. Sci.*, **2014**, *9*, 18.
52. M. M. Momeni, Y. Ghayeb and M. Menati, *J. Mater. Sci. Mater. Electron.*, **2018**, *29*, 4136–4146.
53. M. M. B. El-Sabbah, M. A. Bedair, M. A. Abbas, A. Fahmy, S. Hassaballa and A. A. Moustafa, *Z. Für Phys. Chem.*, **2019**, *233*, 627–649.
54. N. Belarbi, F. Dergal, I. Chikhi, D. Lerari, B. Dahmani, N. Choukchou-Braham and K. Bachari, *Chem. & Chem. Technol.*, **2023**, *17*, 7–17.